Title: Nutritional status and fecundity are synchronised by muscular exopheresis

Authors: Michał Turek[1,2*], Małgorzata Piechota[3†], Nilesh Shanmugam[3†], Marta Niklewicz[3], Konrad Kowalski[3], Agnieszka Chacińska[1,2], Wojciech Pokrzywa[3*]

Affiliations:

[1]*Laboratory of Mitochondrial Biogenesis, Centre of New Technologies, University of Warsaw, Warsaw, Poland.*

[2]*ReMedy International Research Agenda Unit, University of Warsaw, Warsaw, Poland.*

[3]*Laboratory of Protein Metabolism in Development and Aging, International Institute of Molecular and Cell Biology, Warsaw, Poland.*

* Co-corresponding authors

† These authors contributed equally to this work

Correspondence should be directed to:

WP: wpokrzywa@iimcb.gov.pl

MT: m.turek@cent.uw.edu.pl

Abstract

Organismal functionality and reproduction depend on metabolic rewiring and balanced energy resources. However, the crosstalk between organismal homeostasis and fecundity, and the associated paracrine signaling mechanisms are still poorly understood. Using the *Caenorhabditis elegans* we discovered that secretory vesicles termed exophers, attributed in neurons to the removal of neurotoxic components, are released by body wall muscles to support embryonic growth. We found that exopher formation (exopheresis) is a non-cell autonomous process regulated by egg formation in the uterus. Our data suggest that exophers serve as transporters for muscle-generated yolk proteins used for nourishing and improving the growth rate of the next generation. We propose that the primary role of muscular exopheresis is to stimulate the reproductive capacity, thereby influencing the adaptation of worm populations to the current environmental conditions.

Main

The proper cellular function relies on the removal of unwanted contents by proteolysis or degradation mainly via the ubiquitin-proteasome system (UPS) and autophagy[1]. Recently a complementary mechanism was described in *Caenorhabditis elegans*. Under proteotoxic stress, worms' neurons can remove protein aggregates and damaged mitochondria via large membrane-surrounded vesicles called exophers[2]. Waste excretion by exophers in mouse neuronal HT22 cells under oxidative stress conditions was also reported[3]. This extrusion phenomenon could constitute a significant but still poorly explored metabolic waste management pathway. However, not only neurons can remove cellular content via exophers. Using worms expressing fluorescent reporters in the body wall muscle cells (BWM), we identified muscle-derived exophers; these reporters allow simultaneous tracking of proteasomes, closely associated with proteostasis, and mitochondria, which can be extruded in

43 neuronal tissue[2]. Muscular exophers are filled with proteasomes (both 19S and 20S subunits)
44 (**Fig. 1a**), and approximately 12% of them contain mitochondria (**Extended Data Fig. 1**).
45 Muscular exophers are generally more abundant and prominent (with diameters ranging from
46 2 to 15 μm) (**Fig. 1b**) than neuronal exophers[2], and the majority are generated by adult
47 hermaphrodite mid-body muscles (**Fig. 1c**). Exophers are formed in the muscle cell and
48 expelled outside via a pinching off mechanism (**Fig. 1d**). Some exophers that bud off remain
49 connected with the extruding BWM via a thin but elastic tube that permits continued transfer
50 of a large amount of cellular material into the extruded vesicle (**Fig. 1e, Supplementary Video**
51 **1**), similar to neuronal exophers[2]. Proteostasis impairment significantly increases neuronal
52 exopher output[2,3]. In contrast, the number of muscular exophers did not change in response to
53 depletion of the central proteostasis transcription factor HSF-1 (via *hsf-1* RNAi) or to heat
54 stress, and the number increased slightly under conditions of oxidative stress (**Fig. 1f-g**). These
55 observations suggest that proteostasis regulation might be not the core function of muscle
56 exopheresis.

57 Next, we assessed the number of exophers at different time points of the *C.*
58 *elegans* hermaphrodite life cycle. Reminiscent of neuronal exophers, muscular exophers are
59 not produced during the larval stages, and their maximum level is reached around the second
60 and third days of hermaphrodite adulthood (**Fig. 2a**). Because this time point coincides with
61 the worm's maximum reproductive rate, we wondered if reproduction could influence exopher
62 formation. To examine this possibility, we followed exopheresis in males. For the first three
63 days of adulthood, males did not produce any exophers (**Fig. 2a**). This finding suggests that
64 germ cell maturation in the reproductive system of hermaphrodite worms, the process of oocyte
65 fertilization, or embryonic development might regulate muscle exopheresis.

66 To test these hypotheses, we took advantage of a thermosensitive *C. elegans fem-1* mutant
67 strain that does not produce viable sperm at the restrictive temperature of 25 °C. At the
68 permissive temperature of 15 °C, some animals can reproduce as well as wild type
69 hermaphrodites, whereas the rest of the population is sterile[4]. The offspring-producing *fem-*
70 *1* mutant animals grown at 15 °C generated a high number of muscular exophers. Contrarily,
71 animals raised either at 15 °C or 25 °C that were unable to fertilize oocytes did not activate
72 muscular exopheresis (**Fig. 2b-c**), indicating that neither the presence of the female gonad nor
73 the temperature itself were sufficient to trigger exopher release. Notably, hermaphrodites
74 sterilized via fluorodeoxyuridine (FUdR) treatment[5] extruded no exophers or only a few per
75 animal (**Fig. 2d**), suggesting that the occurrence of developing embryos could indeed stimulate
76 muscular exopheresis. We also found that FUdR-treated hermaphrodites often contained
77 exopher-like structures in their BWM (**Fig. 2e**, middle and right panels). Interestingly, we
78 detected objects resembling non-extruded exophers in the BWM of males (**Fig. 2e**, left panel),
79 indicating that males are devoid of mechanisms triggering their expulsion.

80 The above results suggest that the occurrence of developing embryos could induce muscular
81 exopheresis. Consistently, we observed a positive correlation between the number of exophers
82 released and the number of eggs present in the worm uterus (**Fig. 3a**). To further explore this
83 link, we depleted the mRNA of genes responsible for various processes associated with egg-
84 laying. RNAi depletion of the G-protein signalling gene *goa-1* leads to hyperactive egg-laying
85 behaviour, resulting in the presence of fewer early-stage eggs within the uterus[6]. As expected,
86 *goa-1* knockdown caused a significant drop in the level of exopher release. In contrast, the egg-
87 laying defects induced by *egl-1* and *egl-4* RNAi, which lead to egg retention in the uterus[7],
88 increased exopher formation by muscle cells (**Fig. 3b**). In the absence of food, worms halt egg-
89 laying and retain fertilized eggs in the uterus[8,9]; therefore, we anticipated that worms would
90 generate more exophers when experiencing a food shortage. Indeed, the accumulation of

91 developing eggs in the uterus caused by the transfer of adult worms to food-free plates resulted
92 in a significant increase in muscle exopher secretion (**Fig. 3c**). Next, we tested whether worm
93 embryos could directly induce exopher production. We exposed young adult worms to extract
94 from developing eggs from the wild-type strain (**Fig. 3d**). Intriguingly, worms placed in contact
95 with material derived from lysed embryos increased exopheresis by approximately 20% (**Fig.**
96 **3e**). This observation suggests that molecules that diffuse from embryos *in utero* are
97 responsible for exopheresis induction. Finally, we decided to confirm that even in the face of
98 disturbed proteostasis specifically in the BWM, a signal associated with the developing
99 embryos in the uterus would be the primary regulator of muscular exopheresis. To this end, we
100 knocked down the myosin-directed chaperone UNC-45, which results in severe defects in the
101 organization of thick muscle filaments, as well as embryonic defects in cytokinesis and polarity
102 determination[10-12]. We initiated *unc-45* depletion in L4 larvae, which first leads to a disturbance
103 of proteostasis in BWM, and later, in young gravid adults, to inhibition of embryonic
104 development. Despite the dysfunction of a myosin-chaperone network in muscle cells, which
105 was indicated by complete paralysis of worms, we observed a dramatic inhibition of exopher
106 formation (**Fig. 3f**), highlighting the predominant role of maturating eggs in muscular
107 exopheresis.

108 Production of a single exopher involves the elimination of a substantial amount of the muscle
109 cell content. The high number of exophers produced during the *C. elegans* lifespan by BWM
110 leads to the removal of a relatively significant portion of cellular mass by a single tissue. We
111 hypothesized that this process should have substantial effects on worm muscle functionality
112 and healthspan. To this end, we selected three types of worms from the synchronized
113 population of gravid adults based on the number of extruded exophers, i.e., few (< 2), many (>
114 20), and control (6-8) animals (**Fig. 4a**), and analyzed their locomotory behaviour. In neurons,
115 exophers production is correlated with improved cell functionality; however, worms with

116 intensified exopheresis did not show enhanced mobility (**Fig. 4b**, **Extended Data Fig. 2**). On
117 the contrary, these animals displayed a reduction in exploratory behaviour (**Fig. 4c-d**).
118 Furthermore, the active use of muscular exopheresis was correlated with prolonged lifespan,
119 revealing a long-term beneficial effect (**Fig. 4e**).

120 Because, developing embryos stimulate exopher release from the mother BWM, we next
121 wondered whether this process benefited the offspring. Previous work showed that neuronal
122 exopher content can be transported through the worm body to reach distant scavenger cells
123 (coelomocytes)[2]. Moreover, muscle-specific transcriptomic analysis revealed the presence of
124 significant levels of vitellogenin mRNAs (i.e., *vit-2*, *-5* and *-6*)[13]. Therefore, we hypothesized
125 that the components of the yolk from BWM are transported through exophers to be used as a
126 source of raw materials for maturating eggs. To address this possibility, we used RNAi
127 knockdown of *vit-1* (a vitellogenin-coding gene) to reduce the level of the principal yolk
128 protein[14] and investigated whether it led to an increase in exopher biogenesis as a possible
129 compensatory mechanism. Indeed, the number of accumulated muscle-released exophers
130 nearly doubled in response to yolk protein depletion (**Fig. 4f**). Moreover, intensification of
131 exopheresis in the mother increased the amount of vitellogenin in developing eggs (**Fig. 4g**).
132 Next, we followed the localization of vitellogenin-2 (VIT-2) fused to GFP and muscle exopher
133 markers in the hermaphrodite. We detected the presence of VIT-2::GFP in the BWM of day-2
134 adult worms, as well as a significant accumulation in many muscle exophers (**Fig. 4h,**
135 **Extended Data Fig. 3**). These results suggest that exophers can mediate the transport of
136 additional portions of muscle-produced vitellogenin, which is ultimately deposited in oocytes
137 from the body cavity[15]. Finally, we followed the growth of the progeny of hermaphrodites
138 exhibiting different levels of exopheresis (**Fig. 4a**). We found that offspring from mothers with
139 a high number of muscle-released exophers (which showed no change in egg-laying behaviour)

140 grew faster (**Fig. 4i**). This is in line with a previous reports showing that yolk-reach eggs
141 support animals post-embryonic survival and development[14,16,17].

142 **Discussion**

143 We have shown here that muscular exopheresis in *C. elegans* represents a previously
144 uncharacterized nutrient management program associated with nourishing the next generation
145 of worms. The availability of food for mothers affects the number of developing eggs in the
146 uterus and the developmental stage at which the eggs are laid[18]. Activation of exopheresis
147 occurs with the first appearance of developing eggs in the uterus and intensifies in situations
148 of environmental food depletion. Likewise, disturbance of yolk synthesis increases exopher
149 biosynthesis. Consequently, in mothers with highly active exopheresis, the volume of yolk
150 content in eggs increased. Our results show that yolk protein produced in BWM is transferred
151 to exophers and ultimately delivered to oocytes. Therefore, the use of exophers for the transport
152 of vitellogenin represents an elegant mechanism by which remote cells can help to enrich the
153 nourishment of developing embryos. This process leads to the production of larvae that are
154 better prepared to thrive in the current environmental conditions. Thus, muscular exopheresis
155 is likely an adaptive mechanism that affects the dynamics of population growth. The impact of
156 exopheresis on early reproduction may be particularly crucial for wild worms, given the
157 significantly shortened life expectancy observed under more natural conditions[19].
158 Neuronal exopher formation occurs in higher animals[3]. In addition, yolk protein can be
159 synthesized in the muscles of oviparous animals like zebrafish[20], and is supplemented from the
160 mother to the intraovarian embryo in viviparous animals[21]. Hence, it is tempting to speculate
161 that the role of muscular expheresis in supporting progeny development could be evolutionarily
162 conserved. However, the exact mechanisms by which oocyte fertilization and subsequent
163 embryonic development initiate exopher formation and how this exopheresis is executed at the
164 molecular level require further studies.

References

1 Dikic, I. Proteasomal and Autophagic Degradation Systems. *Annu Rev Biochem* **86**, 193-224, doi:10.1146/annurev-biochem-061516-044908 (2017).

2 Melentijevic, I. *et al.* C. elegans neurons jettison protein aggregates and mitochondria under neurotoxic stress. *Nature* **542**, 367-371, doi:10.1038/nature21362 (2017).

3 Hualin, F., Jilong, L., Peng, D., Weilin, J. & Daxiang, C. (bioRxiv, 2019).

4 Nelson, G. A., Lew, K. K. & Ward, S. Intersex, a temperature-sensitive mutant of the nematode Caenorhabditis elegans. *Dev Biol* **66**, 386-409, doi:10.1016/0012-1606(78)90247-6 (1978).

5 Hosono, R. Sterilization and growth inhibition of Caenorhabditis elegans by 5-fluorodeoxyuridine. *Exp Gerontol* **13**, 369-374, doi:10.1016/0531-5565(78)90047-5 (1978).

6 Bany, I. A., Dong, M. Q. & Koelle, M. R. Genetic and cellular basis for acetylcholine inhibition of Caenorhabditis elegans egg-laying behavior. *J Neurosci* **23**, 8060-8069 (2003).

7 Hirose, T. *et al.* Cyclic GMP-dependent protein kinase EGL-4 controls body size and lifespan in C elegans. *Development* **130**, 1089-1099, doi:10.1242/dev.00330 (2003).

8 Daniels, S. A., Ailion, M., Thomas, J. H. & Sengupta, P. egl-4 acts through a transforming growth factor-beta/SMAD pathway in Caenorhabditis elegans to regulate multiple neuronal circuits in response to sensory cues. *Genetics* **156**, 123-141 (2000).

9 Dong, M. Q., Chase, D., Patikoglou, G. A. & Koelle, M. R. Multiple RGS proteins alter neural G protein signaling to allow C. elegans to rapidly change behavior when fed. *Genes Dev* **14**, 2003-2014 (2000).

10 Kachur, T., Ao, W., Berger, J. & Pilgrim, D. Maternal UNC-45 is involved in cytokinesis and colocalizes with non-muscle myosin in the early Caenorhabditis elegans embryo. *J Cell Sci* **117**, 5313-5321, doi:10.1242/jcs.01389 (2004).

11 Gazda, L. *et al.* The myosin chaperone UNC-45 is organized in tandem modules to support myofilament formation in C. elegans. *Cell* **152**, 183-195, doi:10.1016/j.cell.2012.12.025 (2013).

12 Pokrzywa, W. & Hoppe, T. Chaperoning myosin assembly in muscle formation and aging. *Worm* **2**, e25644, doi:10.4161/worm.25644 (2013).

13 Blazie, S. M. *et al.* Comparative RNA-Seq analysis reveals pervasive tissue-specific alternative polyadenylation in Caenorhabditis elegans intestine and muscles. *BMC Biol* **13**, 4, doi:10.1186/s12915-015-0116-6 (2015).

14 Perez, M. F. & Lehner, B. Vitellogenins - Yolk Gene Function and Regulation in. *Front Physiol* **10**, 1067, doi:10.3389/fphys.2019.01067 (2019).

15 Hall, D. H. *et al.* Ultrastructural features of the adult hermaphrodite gonad of Caenorhabditis elegans: relations between the germ line and soma. *Dev Biol* **212**, 101-123, doi:10.1006/dbio.1999.9356 (1999).

16 Van Rompay, L., Borghgraef, C., Beets, I., Caers, J. & Temmerman, L. New genetic regulators question relevance of abundant yolk protein production in C. elegans. *Sci Rep* **5**, 16381, doi:10.1038/srep16381 (2015).

17 Perez, M. F., Francesconi, M., Hidalgo-Carcedo, C. & Lehner, B. Maternal age generates phenotypic variation in Caenorhabditis elegans. *Nature* **552**, 106-109, doi:10.1038/nature25012 (2017).

18 Muschiol, D., Schroeder, F. & Traunspurger, W. Life cycle and population growth rate of Caenorhabditis elegans studied by a new method. *BMC Ecol* **9**, 14, doi:10.1186/1472-6785-9-14 (2009).
19 Van Voorhies, W. A., Fuchs, J. & Thomas, S. The longevity of Caenorhabditis elegans in soil. *Biol Lett* **1**, 247-249, doi:10.1098/rsbl.2004.0278 (2005).
20 Zhong, L. *et al.* Distribution of vitellogenin in zebrafish (Danio rerio) tissues for biomarker analysis. *Aquat Toxicol* **149**, 1-7, doi:10.1016/j.aquatox.2014.01.022 (2014).
21 Iida, A. *et al.* Mother-to-embryo vitellogenin transport in a viviparous teleost. *Proc Natl Acad Sci U S A* **116**, 22359-22365, doi:10.1073/pnas.1913012116 (2019).

221 **Figures**

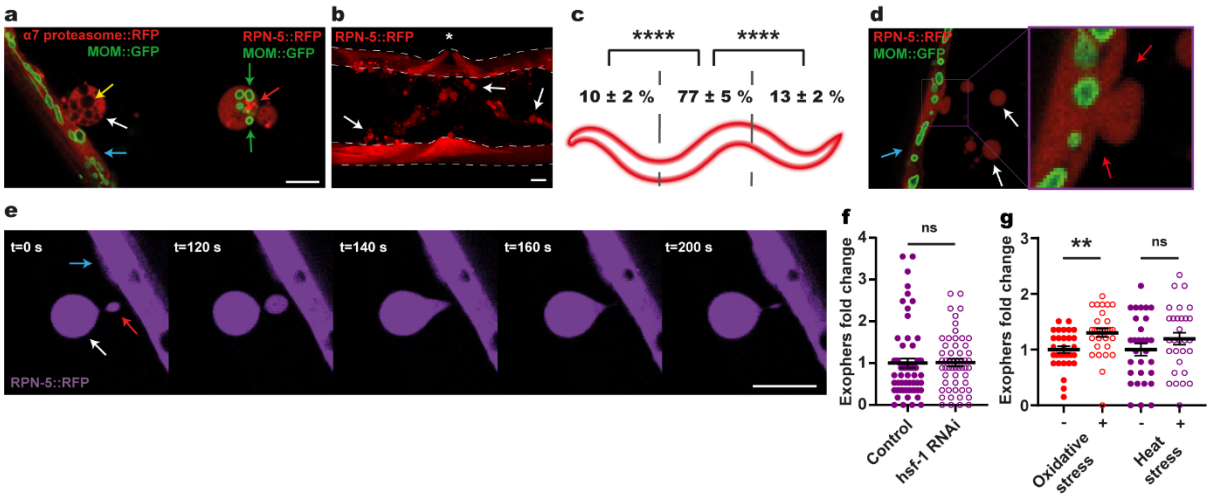

222

223 **Figure 1. *C. elegans* muscles expel cellular content via exophers. a**, Muscular exophers
224 contain organelles and large protein complexes. Arrows: white – exopher, blue – muscle cell,
225 green – mitochondria, red – proteasome foci, yellow – unidentified vesicle. MOM –
226 mitochondrial outer membrane. **b**, BMW actively releases significant amounts of exopher. The
227 image shows the middle part of the worm's body with muscles marked with dashed lines.
228 Arrows indicate representative exophers, and the asterisk indicates the position of the vulva. **c**,
229 Production of muscular exophers is not evenly distributed across all muscle cells. The highest
230 number of exophers is produced by the muscles adjacent to the vulva. n = 46 animals; three
231 biological replicates. **d**, Exophers are formed via a pinching-off mechanism. Arrows: white –
232 exopher, blue – muscle cell, red – distorted muscle cell membrane during exopher formation.
233 **e**, Exophers may remain connected to the sending BWM cells via thin elastic tubes that allow
234 further transfer of cellular material. Arrows: white – exopher, blue – muscle cell, red – cellular
235 material transferred to exopher via elastic tube. **f**, Proteostasis disruption by *hsf-1* knockdown
236 does not increase exopher production. n = 60 and 55 animals, two biological replicates. **g**,
237 Proteostasis induced via oxidative stress but not via heat stress increases exopher production.
238 n = 30 animals; three biological replicates.
239 Scale bars are 10 µm. Data are shown as mean ± SEM. ns – not significant, ** $P < 0.01$, ****
240 $P < 0.0001$; **c**, **f**, **g**, two-tailed Welch's t-test.
241

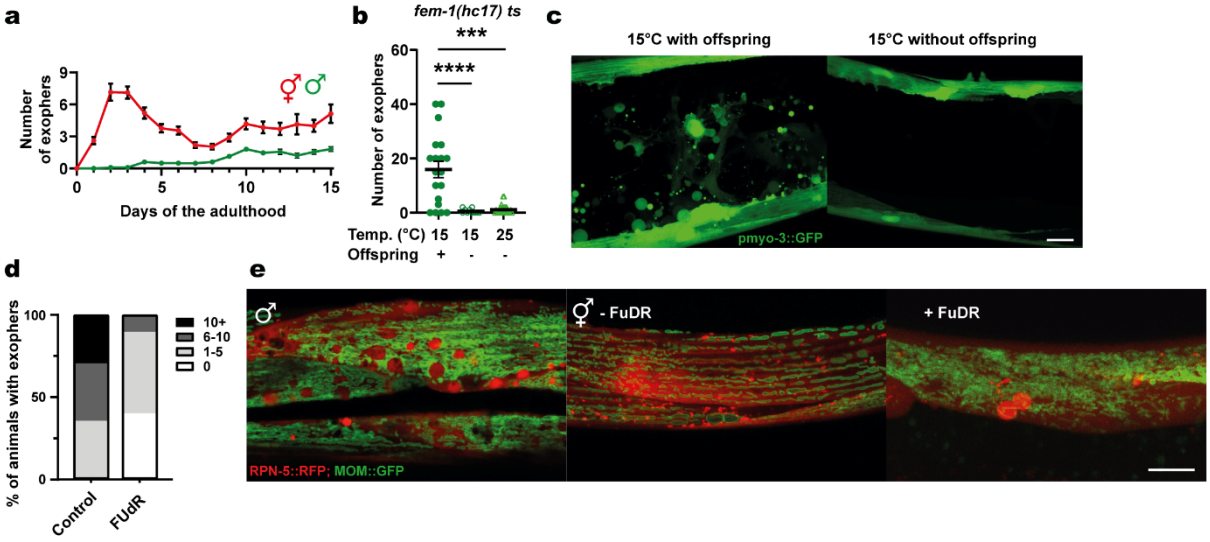

Figure 2. Exopher formation is sex-specific and fertility-dependent. a, The highest number of exophers is produced during the hermaphrodite reproductive period and in aging animals. Males do not produce exophers during the first days of adulthood and begin to generate a small number of exophers later in life. Starting n = 90 hermaphrodites and 150 males; three biological replicates. **b**, Feminized hermaphrodites of thermosensitive a *fem-1* mutant strain do not produce exophers regardless of growth temperature. n = 10 - 26 animals; one biological replicate. **c**, Representative images of the middle part of the worm body in panel b. **d**, Hermaphrodites sterilized via FUdR treatment produce no exophers or only a few per animal. n = 17 and 20 animals; two biological replicates. **e**, Males and sterile hermaphrodites (via FUdR treatment) show the formation of spherical structures in the BWM that resemble mature exophers. MOM – mitochondrial outer membrane.

Scale bars are 10 µm. Data are shown as mean ± SEM; *** $P < 0.001$, **** $P < 0.0001$; **b**, two-tailed Welch's t-test.

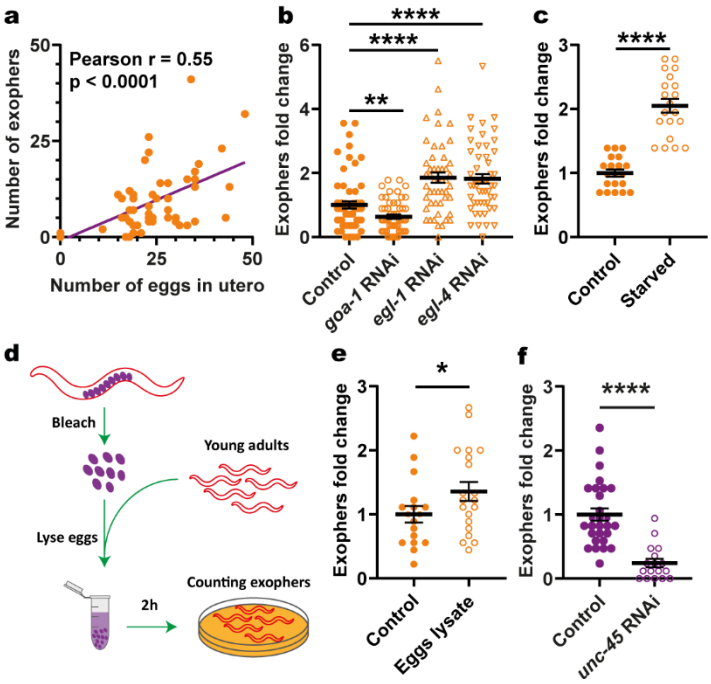

256

257 **Figure 3. Muscular exopheresis is a non-cell autonomous process regulated by *in utero***
258 **developing embryos. a**, The number of produced exophers positively correlates with the
259 number of *in utero* embryos. The violet line is a linear regression line, and each orange point
260 represents one animal. All animals were 1 - 3 days old; n = 54 animals; three biological
261 replicates. **b**, RNAi knockdown of genes regulating the egg laying rate and their presence in
262 the uterus influences exopher production. n = 50 - 60 animals; two biological replicates. **c**, Egg
263 retention in the uterus caused by starvation increases exopher production. n = 20 animals; one
264 biological replicate. **d**, Schematic representation of the experimental setup for investigating the
265 influence of egg lysate on exopher production. **e**, Exposure of young-adult worms to embryo-
266 derived substances increases exopher production. n = 17 and 20 animals; one biological
267 replicate. **f**, RNAi knockdown of the essential muscular co-chaperone *unc-45* reduces exopher
268 production. n = 28 and 17 animals; two biological replicates.
269 Data are shown as mean ± SEM; * P < 0.05, ** P < 0.01, **** P < 0.0001; **b**, **c**, **f**, two-tailed
270 Welch's t-test; **e**, one-tailed Welch's t-test.

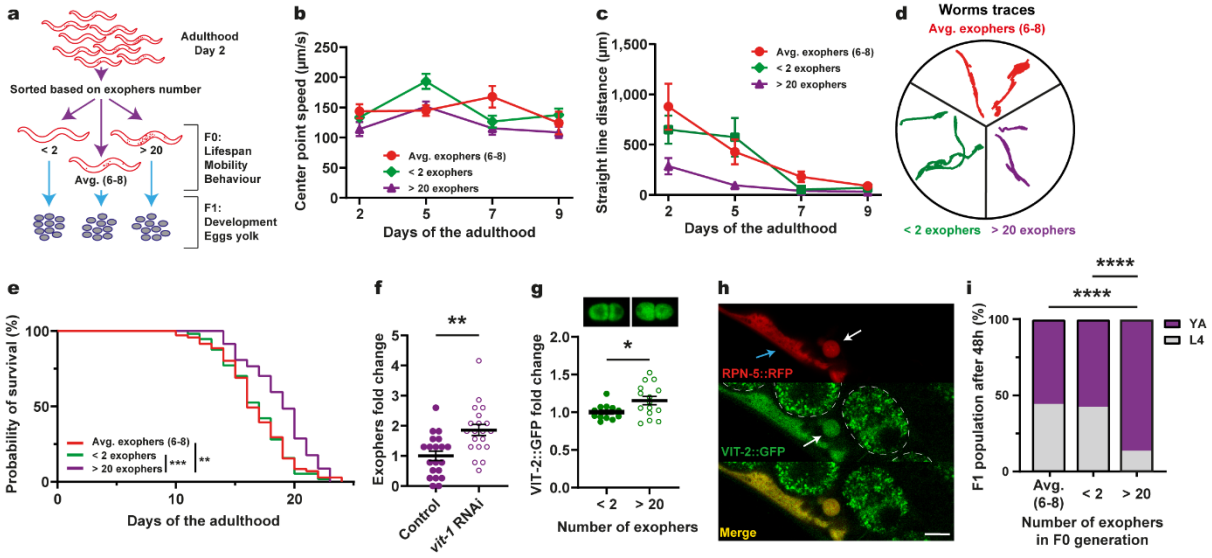

Figure 4. Worms with overactive muscular exopheresis live longer and their offspring develop faster. a, Schematic representation of the experimental setup for investigating the influence of overactive exopheresis on F0 and F1 worm generation. **b**, Exopher production does not improve muscle functionality. n = 11 - 38; three biological replicates. **c-d**, Animals with overactive exopheresis have reduced exploratory behaviour presented as a reduction in straight line distance travelled (c) and by representative worms traces on the plate (d). n = 11 - 34; three biological replicates. **e**, Production of a high number of exophers increases lifespan. n = 63 - 88 animals; three biological replicates. **f**, RNAi knockdown of the egg yolk precursor protein VIT-1 increases the number of muscular exophers. n = 20 animals; two biological replicates. **g**, Embryos from hermaphrodite mothers that produce a high number of exophers contain more egg yolk precursor protein VIT-2. Representative images of embryos with VIT-2::GFP levels from mothers with different exopheresis activity are show above the graph. n = 15 and 14 eggs, five and six biological replicates (animals). **h**, Muscle-produced VIT-2 is released from muscles via exophers. The image shows the midbody of worms expressing the proteasome subunit RPN-5 tagged with RFP in BWM and VIT-2::GFP endogenous expression. Arrows: white – exopher, blue – muscle cell. Dashed lines mark eggs present in the uterus. Scale bar is 10 µm. **i**, Offspring of worms with overactive exopheresis develop faster. YA – young adult stage, L4 – last larval stage. n = 317 – 372 animals; two biological replicates. Data are shown as mean ± SEM. * $P < 0.05$, ** $P < 0.01$, *** $P < 0.001$, **** $P < 0.0001$; **e**, Log-rank (Mantel-Cox) test; **f**, **g**, two-tailed Welch's t-test; **i**, Fisher's exact test.

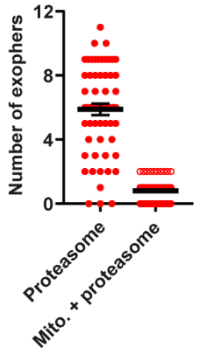

Extended Data Figure 1. Small fraction of muscular exophers contain mitochondria. n = 60; six biological replicates. Data are shown as mean ± SEM.

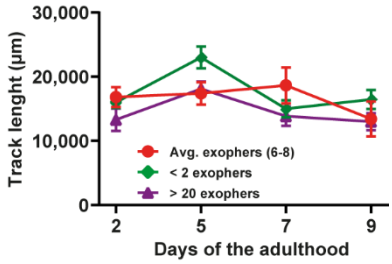

Extended Data Figure 2. Active exophoresis affects worm mobility. Graph shows the track lengths of animals exhibiting different exopheresis activities. n = 11 - 38; three biological replicates. Data are shown as mean ± SEM.

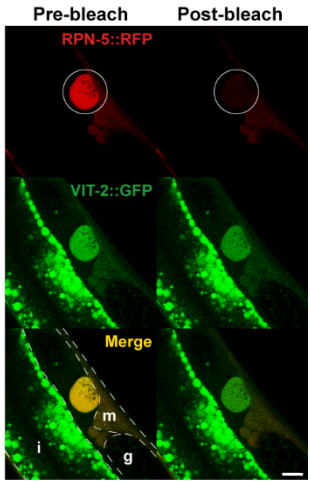

Extended Data Figure 3. Exophers contain muscle-produced vitellogenin. Images show the formation of an exopher filled with the proteasome and vitellogenin. Images were captured before and after RPN-5::RFP photobleaching, confirming that the high signal from VIT-2::GFP in forming exophers is not an imaging artefact. The white circle marks the area that

304 was bleached using a 555 nm laser and the position of developing exopher. Dashed lines mark
305 different tissue borders: m – muscle, i – intestine, g – gonad. Scale bar is 10 µm.

306 **Methods**

307 **Data reporting**

308 No statistical methods were used to predetermine the sample size. The experiments were not
309 randomized. The investigators were not blinded to allocation during experiments and outcome
310 assessment except for lifespan measurement and exploratory behaviour experiments.

311

312 **Worm maintenance and strains**

313 Worms were maintained on Nematode Growing Medium (NGM) plates seeded with
314 OP50 *Escherichia coli* bacteria at 20 °C unless otherwise stated[1]. A list of all strains used in
315 the study, together with the information in which experiments they were used is provided in
316 Supplementary Table 1.

317

318 **Generation of plasmids**

319 All constructs were cloned using the SLiCE method[2] and were sequenced for verification.
320 Construct for the expression of GFP on the mitochondrial outer membrane in the worm's body
321 wall muscles was prepared as follows. First, destination vector pMT26 containing pCG150
322 vector backbone with the *myo-3* promoter and *unc-54* 3'UTR sequences separated by KspAI
323 restriction site was made. Next, codon-optimized sequences[3] for GFP, linker containing attB5
324 sequence, and the sequence of the first 55 amino acids from TOMM-20 protein[4] (from a
325 plasmid that was synthesized for this study) were PCR amplified and inserted into linearized
326 pMT26 vector. To generate construct for expression of RPN-5 or PAS-7 tagged with RFP in
327 worm's body wall muscles, sequences encoding respective proteins were PCR amplified and
328 inserted into pMT26 linearized destination vector. As a template for the *rpn-5*-coding
329 sequence, we used plasmid bearing codon-optimized *rpn-5* cDNA with 3 artificial introns,
330 which was synthesized for this study. The sequence of *pas-7* gene was directly amplified from

331 N2 worms genomic DNA, and the sequence of RFP (wrmScarlet) was amplified from pSEM89
332 plasmid[5].
333
334 **Transgenic strains generation**
335 Worms transgenic strains were created by microparticle bombardment using *unc-*
336 *119(ed3)* rescue as a selection marker[6]. After phenotypic confirmation of successful plasmid
337 insertion, transformants were backcrossed two times against N2 strain to remove the *unc-*
338 *119(ed3)* background.
339
340 **Scoring exophers and Microscopy**
341 For scoring of exophers, a confocal microscope or a stereomicroscope was used.
342 When using the confocal microscope, animals were transferred onto 3 % agarose pads prepared
343 in H_2O and formed on a microscope slide. Next, animals were immobilized on the pad using 6
344 µL of PolySciences 0.05 µm polystyrene microspheres or 25 µM tetramisole and covered with
345 a glass coverslip. Immediately afterward, animals were imaged using an inverted Zeiss
346 LSM800 laser-scanning confocal microscope with 40x or 63x oil immersion objectives. The
347 488 nm and 561 nm lasers were used for excitation of GFP and RFP fluorescent proteins,
348 respectively. Z-stacks, which covered the whole animal, were taken and the number of
349 exophers released by muscles was counted. Finally, data were normalized to the average
350 number of exophers present in control animals and compared between conditions.
351 For scoring exophers with the stereomicroscope, we used Leica M165FC stereomicroscope
352 equipped with Leica EL6000 lamp and standard Texas Red and GFP filter sets. Age
353 synchronized, freely moving, day-2 adult animals were directly visualized on culturing NGM
354 plates and the number of visible exophers released by muscles were counted. Finally, data were

355 normalized to the average number of exophers present in control animals and compared
356 between conditions.
357 Representative pictures of exophers presented in the manuscript were taken with the usage of
358 an inverted Zeiss 700 laser-scanning confocal microscope equipped with a 40x oil objective.
359 The 488 nm and 555 nm lasers were used for excitation of GFP and RFP fluorescent proteins,
360 respectively. To investigate the presence and distribution of exophers, z-stacks were taken and
361 processed with ZEN software.
362
363 **RNA interference**
364 RNA interference in *C. elegans* was performed using the standard RNAi feeding method and
365 RNAi clones[7]. For experiments, we used NGM plates supplemented with 1 mM IPTG and 25
366 µg/µl carbenicillin seeded with HT115 *E. coli* bacteria expressing double-stranded RNA
367 (dsRNA) against the gene of interest or, as a control, with bacteria without a vector. Worms
368 were placed on freshly prepared RNAi plates, either as age-synchronized pretzel-stage eggs,
369 L1 larvae, or L4 larvae. The number of exophers was counted on day 2 adult worms using a
370 confocal microscope or a stereomicroscope.
371
372 **Stress influence on exophers production**
373 Worms were age-synchronized using alkaline hypochlorite solution (bleaching procedure), as
374 previously described[8]. The harvested eggs were incubated overnight at 16 ˚C for hatching.
375 Approx. 1000 L1 larvae were transferred on NGM plates and incubated at 20 °C till they
376 reached day-2 of adulthood. The worms were further channeled to the respective stress
377 treatments.
378 Oxidative stress

379 Approx. 100, day-2 adult worms were washed-off from the NGM plates and rinsed 3 times
380 with M9 buffer. The worms to be stressed were suspended in 1 ml of 5 mM hydrogen peroxide
381 solution prepared in M9 buffer, whereas control worms were suspended in M9 buffer. The
382 tubes were incubated on a shaker at 20 ˚C for 60 minutes.
383 Heat stress
384 Similarly, approx. 100, day-2 adult worms were washed-off form NGM plates and rinsed 3
385 times with M9 buffer. The worms were further suspended in a 1 ml M9 buffer. The worms to
386 be heat stressed were incubated in a shaker at 33 °C for 60 minutes, whereas the control animals
387 were incubated at 20 °C for 60 minutes.
388 Exophers quantification
389 From each stress/control treatment, 30 worms were picked onto agarose pad slides individually
390 for the quantification of exophers. Exophers were quantified using a confocal microscope.
391 Obtained data were normalized to the average number of exophers present in control animals
392 and compared between conditions.
393
394 **Number of exophers on consecutive days**
395 For each biological replicate, 30 L4 larvae hermaphrodites or 50 L4 larvae males were
396 transferred to fresh NGM plates (5 hermaphrodites or 10 males per plate). For the next
397 consecutive 15 days, the number of exophers in each animal was counted using a
398 stereomicroscope. Hermaphrodites were transferred to fresh plates every 2 – 3 days. Males
399 were kept on the same plate until the end of the experiment. All animals that died during the
400 experiment time course were removed from the plate.
401
402 **Measuring exophers in *fem-1* mutant**

403 Approx. 50 L1 larvae from *fem-1(hc17)ts* mutant strain expressing GFP in BWM were
404 transferred to 2 fresh NGM plates. During the time course of the experiment, one of the plates
405 was kept at 15 °C while the second one was kept at 25 °C. When worms reached L4 larval
406 stage, each worm was transferred to a separate plate and grown at the same temperature as
407 before. After 48 hours at 25 °C or 72 hours at 15 °C, using a stereomicroscope, a number of
408 exophers released from worms muscles was counted and plates were scored for F1 offspring
409 to assign all worms as fertile or infertile.
410
411 **FUdR assay**
412 Age-synchronized animals were placed on NGM plates seeded with OP50 *E. coli* bacteria as a
413 food source until they reached young adulthood (day 0). Next, animals were selected and
414 moved to test plates containing 25 μM fluorodeoxyuridine (FUdR) to prevent embryonic
415 development and egg hatching[9] or control plates without FUdR. The number of exophers was
416 counted on adult day-2 using confocal microscopy.
417
418 **Exophers and *in utero* eggs correlation**
419 For correlating the number of exophers with the number of eggs present in worms uterus, 1 to
420 3-days old animals were used. First, muscular exophers for a single worm were counted using
421 the stereomicroscope. Next, worm was transferred to a 10 μl drop of 1.8 % hypochlorite
422 solution put on a microscope slide. Finally, after approx. 5 minutes when the hermaphrodite
423 mother was fully bleached, the number of eggs released from worm's uterus was counted. Data
424 analysis was performed using GraphPad Prism 8 software.
425
426 **Starvation assay**

427 To assess the influence of worms starvation on the exophers production, day-2 adult worms
428 were moved to bacteria-free NGM plates. After 24 hours of food deprivation, the number of
429 exophers was counted using a stereomicroscope. As a control, day-3 adult worms grown for
430 the whole time on NGM plates seeded with bacteria were used. Obtained data were normalized
431 to the average number of exophers present in control animals and compared between
432 conditions.
433
434 **Eggs lysate assay**
435 To obtain eggs, age-synchronized N2 gravid hermaphrodites were bleached using an alkaline
436 hypochlorite solution. Harvested eggs were suspended in appropriate volume of M9 buffer to
437 reach the concentration of approx. 200 eggs per µl. Next, eggs were flash-frozen in liquid
438 nitrogen, thawed on ice, and sonicated 3 times for 10 seconds to obtain eggs lysate. 150 µl of
439 eggs lysate was mixed with 150 µl of concentrated OP50 *E. coli* bacteria and placed in a 0.5
440 ml Eppendorf tube. Approx. 30 day-1 young adult hermaphrodites were transferred to
441 Eppendorf tube containing a mixture of eggs lysate and bacteria and were placed on the rotator
442 for 2 hours at room temperature. After 2 hours, the content of the tube was placed on the fresh
443 NGM plate seeded with OP50 bacteria. 18 hours later the number of exophers in each worm
444 was counted. For control animals, the whole protocol was the same except that for bleaching
445 step no worms were used.
446
447 **Worm exploratory behaviour**
448 Age-synchronized, day-2 adult worms which had an average (6-8), few (< 2), or many (> 20)
449 exophers were sorted to separate NGM plates. Approximately 10 worms per replicate were
450 brought onto NGM plates and the worm movement was recorded for 2 minutes using the
451 WormLab system (MBF Bioscience). The frame rate, exposure time, and gain were set to 7.5

452 frames per second, 0.0031 s, and 1, respectively. The track length, straight-line distance, center
453 point speed, and the overall track pattern of individual worms were analyzed using the
454 WormLab software (MBF Bioscience).
455
456 **Lifespan assay**
457 For each biological replicate, approx. 300 late L4 larvae were transferred to fresh NGM plate.
458 On day 2 of worms' adulthood, the number of exophers in each animal was counted and worms
459 with less than 2 or more than 20 visible exophers were transferred to new plates (25 – 30
460 animals). Additional 25 – 30 worms were picked blindly from the same original population,
461 moved to a fresh plate, and served as a control. Lifespan measurements were performed on
462 these three respective populations. During lifespan measurements, worms were scored daily
463 for movement and pharyngeal pumping until their death. All worms were moved to fresh plates
464 every 1 – 2 days during the eggs-laying period and every 3 – 5 days afterward. Animals that
465 crawled off the plate or exhibited baggy phenotype were censored from the experiment. Data
466 analysis was performed using GraphPad Prism 8 software.
467
468 **Vitellogenin levels in embryos**
469 Vitellogenin levels in embryos were measured based on the GFP signal from fluorescently
470 tagged VIT-2 protein. Approx. 200 late L4 larvae were transferred to fresh NGM plate. On day
471 2 of worms adulthood, the number of exophers in each animal was counted and worms with
472 less than 2 or more than 20 visible exophers were transferred to new plates. Next, animals from
473 each group were individually transferred to a 10 µl drop of M9 buffer which was placed on a
474 microscope slide. Using a sharp injection needle, worm was cut open to release eggs from the
475 uterus. Fluorescent signal from 2-cell embryo stage was captured using Leica M165FC
476 stereomicroscope equipped with Leica EL6000 lamp, standard GFP filter set, and Leica

477 DFC365 FX CCD camera. Magnification used for recording pictures was set to 192x. Exposure
478 time and gain were set to 600 ms and 2, respectively. The fluorescent signal was quantified
479 using Leica Las X software and was normalized to the average signal from eggs, which were
480 obtained from animals with less than 2 exophers.
481
482 **Worms development assay**
483 25 – 30 age-synchronized, day-2 adult worms which had an average (6-8), few (< 2), or many
484 (> 20) exophers were sorted to separate NGM plates. Gravid adults were allowed to lay eggs
485 for 4 hours, afterward removed from the plates, and the development of their offspring was
486 followed. 46 hours later, using the stereomicroscope, developmental stage of each animal was
487 checked, and the proportion between L4 larvae stage worms and young adult worms was
488 calculated.
489
490 **Statistical analysis**
491 Statistical tests used in this study were two-tailed Welch's t-test, one-tailed Welch's t-test, Log-
492 rank (Mantel-Cox) test, and Fisher's exact test. P-value < 0.05 was considered significant.
493
494 **Methods references**
495 1. Brenner, S. The genetics of Caenorhabditis elegans. *Genetics* **77**, 71–94 (1974).
496 2. Zhang, Y., Werling, U. & Edelmann, W. SLiCE: a novel bacterial cell extract-based
497 DNA cloning method. *Nucleic Acids Res.* **40**, e55–e55 (2012).
498 3. Redemann, S. *et al.* Codon adaptation-based control of protein expression in C.
499 elegans. *Nat. Methods* **8**, 250–252 (2011).
500 4. Watanabe, S. *et al.* Protein localization in electron micrographs using fluorescence

501 nanoscopy. *Nat. Methods* **8**, 80–84 (2011).

502 5. El Mouridi, S. *et al.* Reliable CRISPR/Cas9 Genome Engineering in
503 Caenorhabditis elegans Using a Single Efficient sgRNA and
504 an Easily Recognizable Phenotype. *G3 Genes|Genomes|Genetics* **7**, 1429 LP – 1437
505 (2017).

506 6. Praitis, V., Casey, E., Collar, D. & Austin, J. Creation of low-copy integrated
507 transgenic lines in Caenorhabditis elegans. *Genetics* **157**, 1217–1226 (2001).

508 7. Kamath, R. S. & Ahringer, J. Genome-wide RNAi screening in Caenorhabditis
509 elegans. *Methods* **30**, 313–321 (2003).

510 8. Porta-de-la-Riva, M., Fontrodona, L., Villanueva, A. & Cerón, J. Basic Caenorhabditis
511 elegans methods: synchronization and observation. *J. Vis. Exp.* e4019–e4019 (2012).
512 doi:10.3791/4019

513 9. Mitchell, D. H., Stiles, J. W., Santelli, J. & Sanadi, D. R. Synchronous Growth and
514 Aging of Caenorhabditis elegans in the Presence of Fluorodeoxyuridine1. *J. Gerontol.*
515 **34**, 28–36 (1979).

516

517 **Acknowledgements**

518 We thank the Caenorhabditis Genetics Center (funded by the NIH National Center for Research
519 Resources, P40 OD010440) for strains; T. Hoppe for expert advice and Carl Kutzner for RNAi
520 clones; T. Wegierski for confocal microscopy assistance; B. Uszczyńska-Ratajczak, K.
521 Szczepanowska, H. Bringmann, and members of Chacińska and Pokrzywa laboratories for
522 discussions and comments on the manuscript.

523

524

Funding

Work in the W.P. laboratory was supported by the Foundation for Polish Science co-financed by the European Union under the European Regional Development Fund (grant POIR.04.04.00-00-5EAB/18-00 to W.P.), the European Molecular Biology Organization (EMBO Installation Grant No. 3916 to M.P., K.K., and W.P.), the Polish National Science Center (grant UMO-2016/23/B/NZ3/00753 to N.S. and W.P.), and the Deutsche Forschungsgemeinschaft (DFG FOR 2743 to W.P.). Work in the A.C. laboratory was funded by "Regenerative Mechanisms for Health" project MAB/2017/2 (M.T. and A.C.) carried out within the International Research Agendas programme of the Foundation for Polish Science co-financed by the European Union under the European Regional Development Fund and was supported by a POLONEZ Fellowship of National Science Centre, Poland, 2016/21/P/NZ3/03891 (M.T.), within European Union's Horizon 2020 research and innovation programme under the Marie Skłodowska-Curie grant agreement no. 665778.

Author contributions

M.T., W.P., M.P., N.S., M.N., and K.K. conducted and designed experiments, M.T. and W.P. conceived the project and supervised the study. W.P., A.C. and M.T. secured the funding. W.P. and M.T. wrote the manuscript with input from A.C. and M.P

Author Information

The authors declare no competing financial interests. Correspondence and requests for materials should be addressed to M.T., (m.turek@cent.uw.edu.pl) and W.P. (wpokrzywa@iimcb.gov.pl).

550 **Supplementary Information**

551 Supplementary Video 1

552 The video shows the cellular content being transfer from BWM cell to exopher via elastic tube.

553 Supplementary Table 1

554 The file contains a table with the list of all *C. elegans* strains used in this study.

555 Supplementary Table 2

556 The file contains a table with the statistical summary of lifespan experiments

557

558